Journal of Materials Chemistry A

Structure-property relations in Ag-Bi-I compounds: Potential Pb-free absorbers in solar cells

Journal:	*Journal of Materials Chemistry A*
Manuscript ID	TA-ART-11-2018-011227.R1
Article Type:	Paper
Date Submitted by the Author:	18-Jan-2019

Complete List of Authors:	Koedtruad, Anucha; Kyoto University, Institute for Chemical Research Goto, Masato; Kyoto University, Institute for Chemical Research Patino, Midori; Kyoto University, Institute for Chemical Research Tan, Zhenhong; Kyoto University, Institute for Chemical Research Guo, Haichuan; Kyoto University, Institute for Chemical Research Nakamura, Tomoya; Kyoto University, Institute for Chemical Research Handa, Taketo; Kyoto University, Institute for Chemical Research Chen, Wei-tin; National Taiwan University, Center for Condensed Matter Sciences Chuang, Yu-Chun; National Synchrotron Radiation Research Center, Sheu, Hwo-Shuenn; National Synchrotron Radiation Research Center, Science research division Saito, Takashi; Kyoto University, Institute for Chemical Research Kan, Daisuke; Kyoto University, Kanemitsu, Yoshihiko; Institute for Chemical Research, Wakamiya, Atsushi; Kyoto University, Institute for Chemical Research Shimakawa, Yuichi; Kyoto University, Institute for Chemical Research

Journal Name

ARTICLE

Structure-property relations in Ag-Bi-I compounds: Potential Pb-free absorbers in solar cells

Received 00th January 20xx,
Accepted 00th January 20xx

DOI: 10.1039/x0xx00000x

www.rsc.org/

Anucha Koedtruad,[a] Masato Goto,[a] Midori Amano Patino,[a] Zhenhong Tan,[a] Haichuan Guo,[a] Tomoya Nakamura,[a] Taketo Handa,[a] Wei-tin Chen,[b] Yu-Chun Chuang,[c] Hwo-Shuenn Sheu,[c] Takashi Saito,[a] Daisuke Kan,[a] Yoshihiko Kanemitsu,[ad] Atsushi Wakamiya,[ad] Yuichi Shimakawa,*[ad]

Ag-Bi-I system attracts much attention recently as emergent materials for absorbers in solar cells. We have investigated single-phase composition regions in $Ag_{2-3x}Bi_xI_2$, analyzed the detailed crystal structures, measured optical and electronic properties, and revealed the structure-property relations. Single-phase samples with the $CdCl_2$-type rhombohedral structures were obtained at the Ag-rich compositions (x = 0.45−0.48), while the defect-spinel-type cubic structure was stabilized at the Bi-rich compositions (x = 0.52−0.57). Both rhombohedral and cubic structures consist of the cubic close-packed I-ion sublattices, and the small difference in the Ag/Bi composition resulted in the distinct crystal structures. Both $CdCl_2$-type rhombohedral and defect-spinel-type cubic compounds exhibited semiconducting natures with proper band gap energies, which indicates that both materials are potentially useful as absorbers in solar cells. The rhombohedral structure compounds have shallower valence band energies, larger indirect band gap energies, and higher electrical conductivity with lower activation energy than the cubic structure compounds. The distinct properties result from the difference in the defect structures, additional Ag occupation in the rhombohedral phase and the deficiencies of the octahedral site in the cubic phase.

Introduction

Methylammonium lead iodide ($MAPbI_3$) has attracted much attention as an emergent optoelectronic material. One of the most promising applications with the compound is a solar cell. Its power conversion efficiency (PCE) has risen rapidly and now exceeds 22%.[1] Its instability under atmospheric conditions, however, and the high toxicity of the constituent lead are major concerns for commercialization of this material. Accordingly, lead-free materials with high stability in air are strongly demanded and have been extensive attempts to substitute other metals such as Sn, Ge, Sb, and Bi for the Pb in perovskite-related structures. Although a few compounds like $MASnI_3$ and $MAGeI_3$ were found to show photovoltaic properties, good PCE has not been achieved yet.[2-6]

Among such lead-free candidate materials, Bi-containing materials are an interesting class of materials. Some of the halides such as $(CH_3NH_3)_3Bi_2I_9$, $M_3Bi_2I_9$ (M = Cs, Rb, K), $(H_3NC_6H_{12}NH_3)BiI_5$, and $(NH_4)_3Bi_2I_9$ were reported to have band gaps too wide (> 2 eV) for the materials to be used as solar absorbers.[7-10] $AgBi_2I_7$ thin films with the band gap of about 1.87 eV, on the other hand, were recently found to exhibit photovoltaic properties.[11] $AgBiI_4$ was also shown to have an indirect band gap of 1.63 eV with *p*-type low conduction carriers.[12] Exploration for novel halides containing both Ag and Bi has thus accelerated. Although several ternary Ag-Bi-I compounds with nominal compositions of $AgBiI_4$, Ag_2BiI_5, Ag_3BiI_6, and $AgBi_2I_7$ were reported, some of the results are controversial and the chemical composition and crystal structure of each compound have not been clarified in detail.

The AgI-BiI_3 system was first studied by Foucroy, et al., who found that Ag_2BiI_5 and $AgBi_2I_7$ respectively crystalized in the hexagonal and cubic structures.[13] Dzeranova, et al. then reported other two ternary compounds with different compositions, $AgBiI_4$ and Ag_3BiI_6.[14] Odag, et al. analyzed the crystal structures of $AgBiI_4$ and Ag_3BiI_6, synthesized by a solvothermal method, and found that $AgBiI_4$ crystallized in the $Fd\bar{3}m$ cubic and Ag_3BiI_6 crystallized in the $R\bar{3}m$ hexagonal structures.[15] However, they also found significant cation disorder in both compounds, and the refined compositions from the X-ray diffraction (XRD) structure analysis were not consistent with the nominal compositions. The structure-composition relation was thus difficult to establish. The AgI-BiI_3 phase diagram was recently reexamined, and two intermediate phases, γ (based on Ag_2BiI_5) and δ (based on $AgBi_2I_7$), were identified.[16] But the structure-property relationships in the AgI-BiI_3 system have not been established.

In the present study, we have carefully investigated phase relations in Ag-Bi-I compounds with the general formula $Ag_{2-3x}Bi_xI_2$. We have obtained single-phase samples with the $CdCl_2$-type rhombohedral structure and the defect-spinel-type cubic structure and revealed each single phase region. The structural relations

[a] Institute for Chemical Research, Kyoto University, Uji, Kyoto 611-0011, Japan. E-mail (YS): shimak@scl.kyoto-u.ac.jp; Phone: (+81)774-38-3110; Fax: (+81)774-38-3118
[b] Center for Condensed Matter Sciences, National Taiwan University, No. 1, Sec. 4, Roosevelt Road, Taipei 10617, Taiwan
[c] National Synchrotron Radiation Research Center, 101 Hsin-Ann Road, Hsinchu Science Park, Hsinchu 30076, Taiwan
[d] Integrated Research Consortium on Chemical Sciences, Uji, Kyoto 611-0011, Japan

between the two phases are discussed in detail. The measured optical and electrical properties of each single-phase compound are presented and the structure-property relations are also discussed.

Experimental

Compounds with the general formula $Ag_{2-3x}Bi_xI_2$ were prepared by solid-state reaction. The compositions were varied with $0.33 \le x \le 0.60$ to cover the range of compositions of the previously reported compounds (Figure 1). AgI and BiI_3 were well mixed and placed in vacuum-sealed silica tubes, that were then heated in a furnace. The tubes were heated at 610 °C for 1 day, then at 350 °C for 5 days, and then quickly taken out of the furnace.

Phase identification of the obtained samples was performed with a conventional XRD method. Detailed crystal structures were analyzed by using synchrotron XRD (SXRD) data. The SXRD measurements at room temperature were conducted at the beamline BL02B2 in SPring-8 with a wavelength of 0.5996871 Å and at the TPS09A beamline in Taiwan photon source with a wavelength of 0.61992 Å. Powder samples were packed into a 0.1 mm glass capillary tube to minimize absorption and were rotated during the measurement. The obtained data were analyzed with the Rietveld method using the program RIETAN-VENUS.[17]

The optical properties of each single-phase sample were analyzed with photoelectron spectroscopy data and UV-visible absorption spectroscopy data. Valence band energy (E_v) levels of the samples were determined by measuring photoelectron spectra. The powder samples were put into sample holders and exposed to 10 nW light. The spectra were recorded in the range of 4−7 eV. Optical band gaps (E_g) were measured by UV-visible spectroscopy. Samples consisting of a small amount of powder dispersed on glass slides were exposed to light in the energy (E) range from 0.99 to 3.10 eV to measure reflectance (R) and transmittance (T). Absorbance (A) was calculated from $A = -\log(T/(1-R))$. The obtained spectra were analyzed by using Tauc plots, $(A*E)^r$ vs. E.

AC electrical conductivity at a fixed frequency of 100 kHz was measured with a circular pellet, 10 mm in diameter and 1.3 mm thick. Conducting silver paint was used as electrodes. The measurements were performed under N_2 gas to temperature at 100 °C in a rate of ~1 °C/min.

Results and discussion

SXRD patterns of the synthesized samples are shown in Figure 2. The results show that single-phase samples were obtained in the composition ranges of $0.45 \le x \le 0.48$ and $0.52 \le x \le 0.57$. The diffraction pattern of each sample with $0.45 \le x \le 0.48$ is indexed with a rhombohedral unit cell. Samples with $0.33 \le x < 0.45$ contain AgI in addition to the rhombohedral phase. For $0.52 \le x \le 0.57$, on the other hand, another single-phase diffraction pattern, which is reproduced by a cubic structure model, appears. For the further Bi-rich composition range ($0.57 < x$), BiI_3 is included and it was difficult to obtain single-phase samples. The results indicate that there are no single phases with nominal compositions Ag_3BiI_6 ($x = 0.33$), Ag_2BiI_5 ($x = 0.40$), and $AgBiI_4$ ($x = 0.50$), which were reported previously, and only $AgBi_2I_7$ ($x = 0.57$) gave the single phase diffraction pattern. The present results are in agreement with the phase diagram reported by Mashadieva, et al., where only γ (based on Ag_2BiI_5) or δ (based on $AgBi_2I_7$) phases exist in the composition range.[16] It can thus be concluded that Ag-rich compositions stabilize the rhombohedral structure, while Bi-rich compositions stabilize the cubic one.

The crystal structures of the obtained single phase samples were then analyzed by the Rietveld method with the SXRD data. Figure 3 shows typical examples of the results for the rhombohedral phase ($x = 0.45$; $Ag_{0.65}Bi_{0.45}I_2$) and the cubic phase ($x = 0.55$; $Ag_{0.35}Bi_{0.55}I_2$). Their refined structure parameters are listed in Table 1. The observed diffraction pattern of $Ag_{0.65}Bi_{0.45}I_2$ is well reproduced with a $CdCl_2$-type crystal structure model with the space group $R\bar{3}m$. The structure consists of a cubic close-packed I-ion sublattice as shown in Figure 4. Ag and Bi ions occupy the 3*a* edge-sharing octahedral sites, and the site is fully occupied with the refined occupancies of Ag/Bi = 0.554(4)/0.446(4). Because no superstructure reflections were observed in the diffraction of these compounds, there was no ordering of Ag and Bi ions at the site. A small amount of Ag occupation (0.070(3)) is detected at the 3*b* sites in the refinement. The refined composition from the structure analysis is $Ag_{0.624}Bi_{0.446}I_2$, which agrees well with the synthesis composition. The (Ag/Bi)-I bond length in the octahedron is 3.0786(7) Å, which is smaller than the expected lengths of ionic bonds consisted of Ag^+ (1.15 Å), Bi^{3+} (1.03 Å), and I^- (2.2 Å), suggesting a covalent nature of the compound. The length of the Ag(3*b*)-I bond sandwiched by the $(Ag/Bi)I_6$ octahedral layers is 3.0373(6) Å, which is slightly less than that of the (Ag/Bi)-I bond. The diffraction pattern of $Ag_{0.35}Bi_{0.55}I_2$, on the other hand, is reproduced with a cubic spinel-type structure model with the space group $Fd\bar{3}m$. This structure is also based on the cubic close-packed I-ion sublattice along the cubic [1 1 1] direction. Note that the tetrahedral site in the spinel structure is completely vacant, indicating the defect-type one. Both Ag and Bi ions occupy the 16*c* edge-sharing octahedral sites, but the total occupancy of the site is less than unity (~0.91), indicating the cation deficiency at the site. No ordering of Ag and Bi ions is confirmed. The refined composition is $Ag_{0.3537}Bi_{0.5558}I_2$, which is also consistent with the synthesis composition. The (Ag/Bi)-I bond length in the edge-sharing octahedron is 3.0835(5) Å, which is slightly greater than that in the rhombohedral phase.

It is interesting to note that the tetrahedral site in the spinel-type structure is completely vacant. Because the Ag^+ and Bi^{3+} ions are too large to occupy the site, $Ag_{2-3x}Bi_xI_2$ cannot crystallize in the spinel-type structure when $x < 0.5$. On the other hand, the octahedral 3*b* site in the $CdCl_2$-type structure is large enough to accommodate the Ag^+ and Bi^{3+} ions. $Ag_{2-3x}Bi_xI_2$ ($x < 0.5$) thus crystallizes in the $CdCl_2$-type structure. The phase transformation in the $Ag_{2-3x}Bi_xI_2$ system is therefore a size effect with the phase boundary at about $x = 0.5$.

Typical photoelectron spectroscopy results are shown in Figure 5, and E_v levels obtained from the single-phase samples are summarized in Table 2. E_v levels for the rhombohedral phase are −6.12 ~ −6.13 eV, while those for the cubic phase are −6.36 ~ −6.41 eV. As shown in the UV-visible absorption spectra in Figure 6, the

rhombohedral phase shows an absorption onset at around 1.5 eV. The relatively steep and significant increase at the onset energy ~1.5 eV is quite suitable for photovoltaic applications. The cubic phase, on the other hand, exhibits two absorption onsets, at ~1.2 and ~1.7 eV. The high energy absorption onset ~1.7 eV is close to the experimentally observed values reported previously.[11,12,18-19] The observed low energy absorption ~1.2 eV in the cubic phase can be assigned to an indirect band gap energy or defect states. Given the indirect band gaps for the present $Ag_{2-3x}Bi_xI_2$ system,[20-21] the Tauc plot analyses $(A*E)^{0.5}$ vs. E give the energies of 1.50 eV for the rhombohedral phase and 1.11 eV for the cubic phase. The results for the other single-phase samples are listed in Table 2, and it can be concluded that indirect band gap energies of the rhombohedral phase are larger than those of the cubic phase.

Note that despite the varying of the Ag and Bi composition ratio, both valence band and band gap energies of each phase change little. This implies that the difference in the optical properties mainly originates from the difference in the crystal structure between the rhombohedral and cubic phases. The valence bands of the compounds mainly consist of Ag-4*d* and I-5*p* states,[12] and the contribution from the Ag(3*b*)-I bonds makes the valence band energy increase, giving a slightly shallower valence band level for the rhombohedral phase. The smaller indirect band gap energies for the cubic phase should be related to the deficiency at the 16*c* edge-sharing octahedral site. A similar absorption onset was indeed reported in $M_3Bi_2I_9$ (M^+ = K^+, Rb^+, Cs^+, NH_4^+, $CH_3NH_3^+$) with cation-deficient BiI_6 octahedral sites.[8,22-26]

The AC electrical conductivity of each single-phase sample increases with increasing temperature, suggesting semiconducting properties of the materials, which is consistent with the UV-visible spectroscopy results. Although possible ionic conduction may be included in the conductivity behavior, the observed property at the measured temperature range essentially originates from the electronic conduction. The phase stability after the conductivity measurements was also confirmed. Actually, each structure phase is stable up to ~130 °C, which we also confirmed from the temperature variable XRD measurements (data are not shown). The conductivity of the rhombohedral $Ag_{0.65}Bi_{0.45}I_2$ is higher than that of the cubic $Ag_{0.35}Bi_{0.55}I_2$. The Arrhenius plots for the temperature dependence of conductivity are shown in Figure 7. The activation energy for the rhombohedral $Ag_{0.65}Bi_{0.45}I_2$ obtained from the plots (10.89 kJ/mol) is lower than that for the cubic $Ag_{0.35}Bi_{0.55}I_2$ (25.77 kJ/mol). The shallower valence band level for the rhombohedral phase lowers activation energy for the electron hopping, making the conductivity higher than that of the cubic phase. Cation defects in the three-dimensional network of the spinel crystal structure may prevent the high conduction of the hopping electrons. The phase stability after the conductivity measurements was also confirmed from the XRD results.

Conclusions

We have prepared $Ag_{2-3x}Bi_xI_2$ (x = 0.33–0.60) by solid-state reactions and investigated the composition-structure relation. We found from the SXRD analysis that the Ag-rich compositions yielded the rhombohedral phase and the single phase was obtained in the composition range of $0.45 \le x \le 0.48$, while the Bi-rich compositions yielded the cubic phase and the single phase was obtained with $0.52 \le x \le 0.57$. The rhombohedral phase crystallized in the $CdCl_2$-type $R\bar{3}m$ crystal structure. The Ag and Bi ions fully occupied the edge-sharing octahedral sites in a disordered manner and additional Ag ions occupied the sites between the $(Ag/Bi)I_6$ octahedral layers. The cubic phase had the cubic defect-spinel-type $Fd\bar{3}m$ crystal structure, where the tetrahedral sites were completely vacant and the Ag and Bi ions partially occupied the edge-sharing octahedral sites. Both structures consisted of the cubic close-packed I-ion sublattices, and thus the small difference in the Ag/Bi composition resulted in the distinct crystal structures.

Both rhombohedral and cubic $Ag_{2-3x}Bi_xI_2$ exhibited semiconducting natures with indirect band gaps. The rhombohedral structure compounds had shallower valence band energies, larger indirect band gaps, and higher electrical conduction with lower activation energies than the cubic structure compounds. The defect structures like additional Ag occupation in the rhombohedral phase and the deficiencies of the octahedral site in the cubic phase played important roles in the distinct properties.

Both $CdCl_2$-type rhombohedral structure compounds and defect-spinel-type cubic structure compounds are potentially useful as absorbers in solar cells. Comparing the properties between the present single-phase samples reveals that the Ag-rich composition rhombohedral compounds would be better absorbers than the Bi-rich composition cubic compounds.

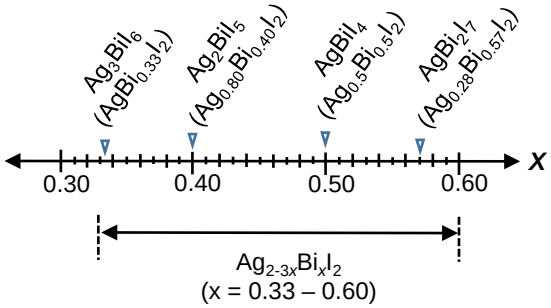

Figure 1. Composition range studied in the present work. Compounds with specific nominal compositions reported previously are also shown.

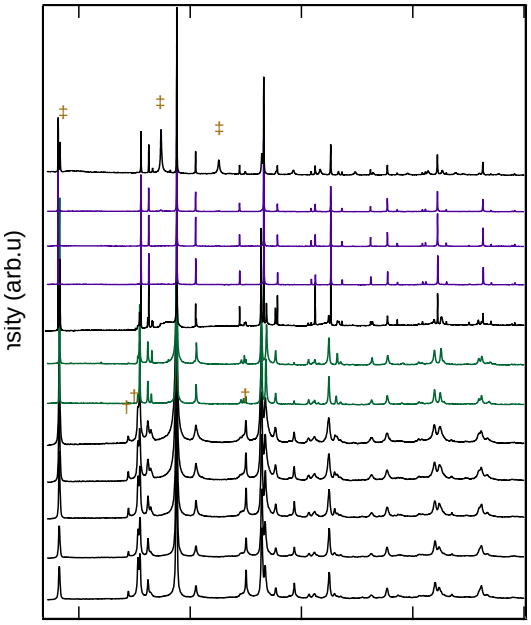

Figure 2. SXRD patterns of $Ag_{2-3x}Bi_xI_2$ (x = 0.33 – 0.60). Diffraction peaks of the impurity phases are indicated with † = AgI and ‡ = BiI_3.

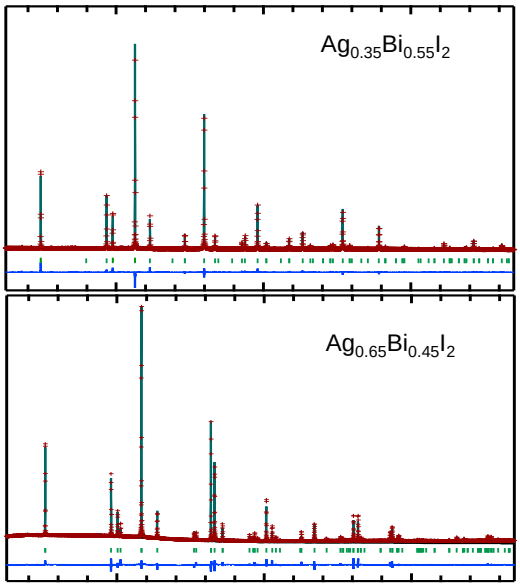

Figure 3. SXRD patterns and the results of structure analysis for $Ag_{0.65}Bi_{0.45}I_2$ with the $CdCl_2$-type rhombohedral structure and $Ag_{0.35}Bi_{0.55}I_2$ with the defect-spinel-type cubic structure. The red marks and green solid line represent observed and calculated patterns, respectively. The blue line below is the difference between the observed and calculated intensities. The ticks are the allowed Bragg reflection positions.

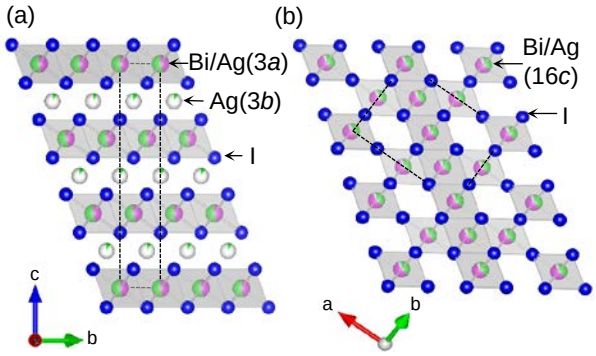

Figure 4. Crystal structures of (a) $CdCl_2$-type rhombohedral phase and (b) defect-spinel-type cubic phase. The green, pink, and blue spheres represent Ag^+, Bi^{3+}, and I^- ions, respectively.

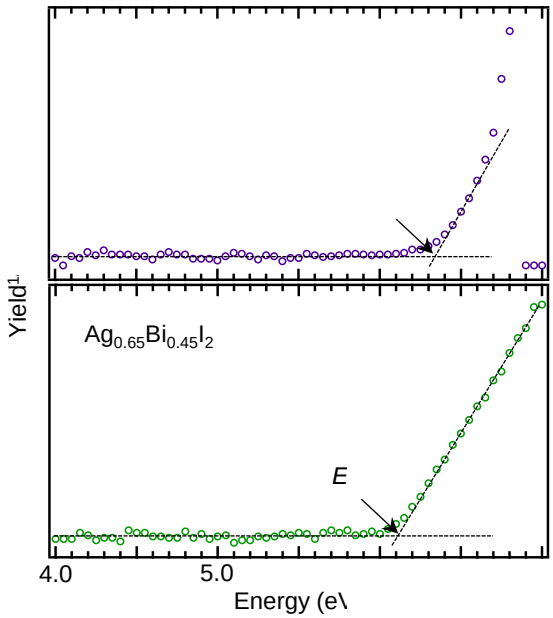

Figure 5. Photoelectron spectra of rhombohedral $Ag_{0.65}Bi_{0.45}I_2$ and cubic $Ag_{0.35}Bi_{0.55}I_2$.

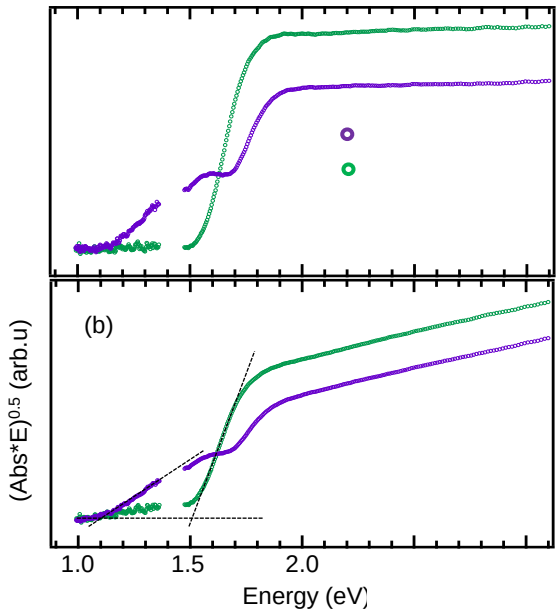

Figure 6. (a) Absorption spectra of rhombohedral $Ag_{0.65}Bi_{0.45}I_2$ and cubic $Ag_{0.35}Bi_{0.55}I_2$ and (b) the corresponding Tauc plot assuming an indirect transition. The dotted lines are the linear extrapolation, and the extrapolated indirect band gap energies are listed in Table. 2. The data at 1.36 - 1.47 eV is missing due to the measurement detector change.

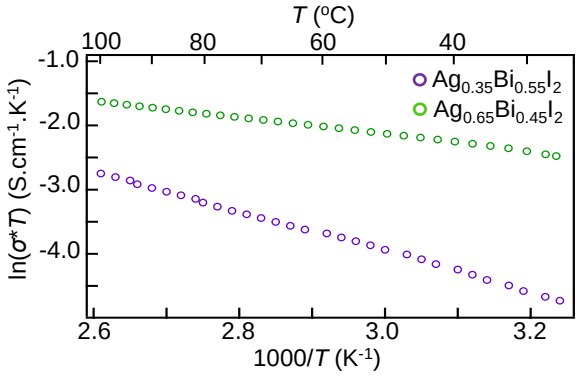

Figure 7. Arrhenius plots of AC electrical conductivity of rhombohedral $Ag_{0.65}Bi_{0.45}I_2$ and cubic $Ag_{0.35}Bi_{0.55}I_2$.

Table 1 Refined structure parameters obtained from room-temperatuure SXRD data for $Ag_{0.65}Bi_{0.45}I_2$ and $Ag_{0.35}Bi_{0.55}I_2$.

Atom	*Site*	*x*	*y*	*z*	*g*	*B* (Å²)
$Ag_{0.65}Bi_{0.45}I_2$[a]						
Ag1	3*a*	0	0	0	0.569(2)	4.32(4)
Ag2	3*b*	0	0	0.5	0.081(2)	3.9(6)
Bi	3*a*	0	0	0	0.431(2)	4.32(4)
I	6*c*	0	0	0.24827(5)	1.0	2.78(3)
$Ag_{0.35}Bi_{0.55}I_2$[b]						
Ag	16*c*	0	0	0	0.3537(5)	3.88(2)
Bi	16*c*	0	0	0	0.5558(5)	3.88(2)
I	32*e*	0.25248(4)	0.25248(4)	0.25248(4)	1.000	2.52(1)

g is a site occupancy and *B* is an isotropic thermal parameter.

[a] Crystal structure; rhombohedral, $R\bar{3}m$ space group, *a*=4.35553(3) Å, *c*=20.8765(1) Å, *V*=342.981(3) Å³, R_{wp} = 3.975%, and R_p =2.411%.

[b] Crystal structure; cubic, $Fd\bar{3}m$ space group, *a*=12.21150(3) Å, *V* = 1820.987(7) Å³, R_{wp} = 4.906%, and R_p =3.570%

Table 2 Valence band level, indirect band gap, and activation energy of the single-phase rhombohedral and cubic compounds.

Samples	Valence band level (eV)	Indirect band gap (eV)	Activation energy (kJ/mol)
Rhombohedral			
$Ag_{0.65}Bi_{0.45}I_2$	-6.12 ± 0.03	1.50	10.89
$Ag_{0.55}Bi_{0.48}I_2$	-6.13 ± 0.04	1.53	15.41
Cubic			
$Ag_{0.44}Bi_{0.52}I_2$	-6.38 ± 0.01	1.08	28.32
$Ag_{0.35}Bi_{0.55}I_2$	-6.36 ± 0.04	1.11	25.77
$Ag_{0.28}Bi_{0.57}I_2$	-6.41 ± 0.04	1.10	27.21

Conflicts of interest

There are no conflicts to declare.

Acknowledgements

The synchrotron radiation experiments were performed at the Japan Synchrotron Radiation Research Institute, Japan (proposal Nos: 2017A1823, 2017B1834, 2017B1643, and 2018B1710) and the National Synchrotron Radiation Research Center, Taiwan (proposal Nos: 2017-1-125). This work was supported by Grant-in-Aid for Scientific Research (Nos: 16H02266) and by a grant for the Integrated Research Consortium on Chemical Sciences from the Ministry of Education, Culture, Sports, Science and Technology (MEXT) of Japan. This work was also partly supported by Japan Society for the Promotion of Science (JSPS) Core- to-Core Program (A) Advanced Research Networks and Japan Science and Technology Agency's ALCA (JPMJAL1603) and CREST (JPMJCR16N3) programs.

References

1 W. S. Yang, B. W. Park, E. H. Jung, N. J. Jeon, Y. C. Kim, D. U. Lee, S. S. Shin, J. Seo, E. K. Kim, J. H. Noh and S. Il Seok, *Science.*, 2017, **356**, 1376–1379.

2 N. K. Noel, S. D. Stranks, A. Abate, C. Wehrenfennig, S. Guarnera, A. A. Haghighirad, A. Sadhanala, G. E. Eperon, S. K. Pathak, M. B. Johnston, A. Petrozza, L. M. Herz and H. J. Snaith, *Energy Environ. Sci.*, 2014, **7**, 3061–3068.

3 J. Liu, M. Ozaki, S. Yakumaru, T. Handa, R. Nishikubo, Y. Kanemitsu, A. Saeki, Y. Murata, R. Murdey and A. Wakamiya, *Angew. Chemie - Int. Ed.*, 2018, **57**, 13221–13225.

4 Z. Xiao, W. Meng, J. Wang, D. B. Mitzi and Y. Yan, *Mater. Horizons*, 2017, **4**, 206–216.

5 T. Krishnamoorthy, H. Ding, C. Yan, W. L. Leong, T. Baikie, Z. Zhang, M. Sherburne, S. Li, M. Asta, N. Mathews and S. G. Mhaisalkar, *J. Mater. Chem. A*, 2015, **3**, 23829–23832.

6 I. Kopacic, B. Friesenbichler, S. F. Hoefler, B. Kunert, H. Plank, T. Rath and G. Trimmel, *ACS Appl. Energy Mater.*, 2018, **1**, 343–347.

7 B. W. Park, B. Philippe, X. Zhang, H. Rensmo, G. Boschloo and E. M. J. Johansson, *Adv. Mater.*, 2015, **27**, 6806–6813.

8 A. J. Lehner, D. H. Fabini, H. A. Evans, C. A. Hébert, S. R. Smock, J. Hu, H. Wang, J. W. Zwanziger, M. L. Chabinyc and R. Seshadri, *Chem. Mater.*, 2015, **27**, 7137–7148.

9 D. M. Fabian and S. Ardo, *J. Mater. Chem. A*, 2016, **4**, 6837–6841.

10 S. Sun, S. Tominaka, J. H. Lee, F. Xie, P. D. Bristowe and A. K. Cheetham, *APL Mater.*, 2016, **4**, 031101.

11 Y. Kim, Z. Yang, A. Jain, O. Voznyy, G. H. Kim, M. Liu, L.

N. Quan, F. P. García de Arquer, R. Comin, J. Z. Fan and E. H. Sargent, *Angew. Chemie - Int. Ed.*, 2016, **55**, 9586–9590.

12 H. C. Sansom, G. F. S. Whitehead, M. S. Dyer, M. Zanella, T. D. Manning, M. J. Pitcher, T. J. Whittles, V. R. Dhanak, J. Alaria, J. B. Claridge and M. J. Rosseinsky, *Chem. Mater.*, 2017, **29**, 1538–1549.

13 P. H. Fourcroy, M. Palazzi, J. Rivet, J. Flahaut and R. Céolin, *Mater. Res. Bull.*, 1979, **14**, 325–328.

14 K. B. Dzeranova, N. I. Kaloev and G. A. Bulakhova, *Zhurnal Neorg. Khimii*, 1985, **30**, 2983–2985.

15 T. Oldag, T. Aussieker, H. L. Keller, C. Preitschaft and A. Pfitzner, *Z. Anorg. Allg. Chem.*, 2005, **631**, 677–682.

16 L. F. Mashadieva, Z. S. Aliev, A. V. Shevelkov and M. B. Babanly, *J. Alloys Compd.*, 2013, **551**, 512–520.

17 F. Izumi and K. Momma, *Solid State Phenom.*, 2007, **130**, 15–20.

18 H. Zhu, M. Pan, M. B. Johansson and E. M. J. Johansson, *ChemSusChem*, 2017, **10**, 2592–2596.

19 I. Turkevych, S. Kazaoui, E. Ito, T. Urano, K. Yamada, H. Tomiyasu, H. Yamagishi, M. Kondo and S. Aramaki, *ChemSusChem*, 2017, **10**, 3754–3759.

20 Z. Shao, T. Le Mercier, M. B. Madec and T. Pauporté, *Mater. Des.*, 2018, **141**, 81–87.

21 B. Ghosh, B. Wu, X. Guo, P. C. Harikesh, R. A. John, T. Baikie, A. T. S. Wee and C. Guet, 2018, **1802051**, 1–7.

22 R. L. Z. Hoye, R. E. Brandt, A. Osherov, V. Stevanovic, S. D. Stranks, M. W. B. Wilson, H. Kim, A. J. Akey, J. D. Perkins, R. C. Kurchin, J. R. Poindexter, E. N. Wang, M. G. Bawendi, V. Bulovic and T. Buonassisi, *Chem. - A Eur. J.*, 2016, **22**, 2605–2610.

23 X. Huang, S. Huang, P. Biswas and R. Mishra, *J. Phys. Chem. C*, 2016, **120**, 28924–28932.

24 M. Pazoki, M. B. Johansson, H. Zhu, P. Broqvist, T. Edvinsson, G. Boschloo and E. M. J. Johansson, *J. Phys. Chem. C*, 2016, **120**, 29039–29046.

25 Y. Zhang, J. Yin, M. R. Parida, G. H. Ahmed, J. Pan, O. M. Bakr, J. L. Brédas and O. F. Mohammed, *J. Phys. Chem. Lett.*, 2017, **8**, 3173–3177.

26 R. D. Nelson, K. Santra, Y. Wang, A. Hadi, J. W. Petrich and M. G. Panthani, *Chem. Commun.*, 2018, **54**, 3640–3643.

Journal Name

ARTICLE

Table of contents

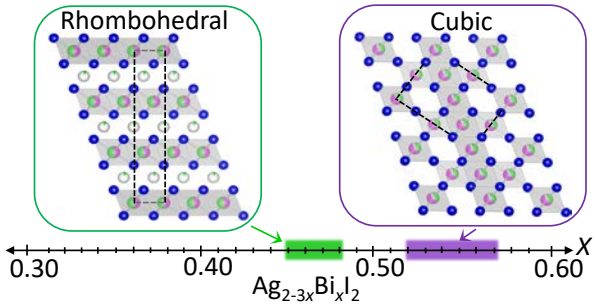

Single phase samples of $Ag_{2-3x}Bi_xI_2$ were obtained and the structure-property relations have been revealed.